AR-010-543

Stress Concentration Around a Patched Hole in an Axi-Symmetrically Loaded Plate

C. Pickthall and L.R.F. Rose

DSTO-RR-0132

19980909 072

APPROVED FOR PUBLIC RELEASE

© Commonwealth of Australia

DTIC QUALITY INSPECTED 1

DEPARTMENT ◆ OF DEFENCE

DEFENCE SCIENCE AND TECHNOLOGY ORGANISATION

AQF98-12-2381

Stress Concentration Around a Patched Hole in an Axi-Symmetrically Loaded Plate

C. Pickthall and L. R. F. Rose

Airframes and Engines Division
Aeronautical and Maritime Research Laboratory

DSTO-RR-0132

ABSTRACT

This paper examines the efficiency of an adhesively bonded reinforcement patch in reducing the stress concentration around a hole in a plate, as a function of hole size. Differential equations are derived for the radial and tangential displacements in the plate and reinforcement assuming only in-plane stresses without out-of-plane bending. Imposition of angular independence leads to distinct load transfer lengths for radial and tangential adhesive shear (β_r^{-1} and β_θ^{-1} respectively), and zero tangential displacement reduces the problem to a patched circular hole with axi-symmetric loading. Four boundary conditions permitted analytic solutions in terms of modified Bessel functions. A stress concentration factor (*SCF*) is defined as the tangential stress in the plate at the hole boundary, compared to that far away in the plate but still under the reinforcement. Plotting *SCF* against hole radius normalised by β_r^{-1}, leads to an analytic function with a single (non-dimensional) parameter *h*, depending on the thicknesses and moduli of the components. *SCF* approaches two in the limit of small holes indicating that the reinforcement is ineffective in that limit. *SCF* approaches $1/h$ in the large-hole limit. For the typical repair geometry where $h \approx 1$, *SCF* falls to 1.6 when the hole radius reaches β_r^{-1}, and 1.3 by $3\beta_r^{-1}$. The related problem of a circular reinforcement bonded on a large (unholed) plate is briefly examined. This indicates how the normalisation stress for *SCF* relates to that applied beyond the patch.

RELEASE LIMITATION

Approved for public release

DEPARTMENT OF DEFENCE

DEFENCE SCIENCE AND TECHNOLOGY ORGANISATION

Published by

DSTO Aeronautical and Maritime Research Laboratory
PO Box 4331
Melbourne Victoria 3001

Telephone: (03) 9626 7000
Fax: (03) 9626 7999
© *Commonwealth of Australia 1998*
AR No. 010-543
May 1998

APPROVED FOR PUBLIC RELEASE

Stress Concentration Around a Patched Hole in an Axi-Symmetrically Loaded Plate

Executive Summary

This paper examines the efficiency of an adhesively bonded reinforcement patch in reducing the stress concentration around a hole in a plate, as a function of hole size. This problem is of interest particularly in the context of battle damage repair, where irregular damage zones are often cut out to a circular shape prior to repair.

Differential equations are derived for the radial and tangential displacements in the plate and reinforcement assuming only in-plane stresses without out-of-plane bending. Imposition of angular independence leads to distinct load transfer lengths for radial and tangential adhesive shear (β_r^{-1} and β_θ^{-1} respectively), and zero tangential displacement reduces the problem to a patched circular hole with axi-symmetric loading. Four boundary conditions permitted analytic solutions in terms of modified Bessel functions. A stress concentration factor (*SCF*) is defined as the tangential stress in the plate at the hole boundary, compared to that far away in the plate but still under the reinforcement. Plotting *SCF* against hole radius normalised by β_r^{-1}, leads to an analytic function with a single (non-dimensional) parameter h, depending on the thicknesses and moduli of the components. *SCF* approaches two in the limit of small holes indicating that the reinforcement is ineffective in that limit. *SCF* approaches $1/h$ in the large-hole limit. For the typical repair geometry where $h \approx 1$, *SCF* falls to 1.6 when the hole radius reaches β_r^{-1}, and 1.3 by $3\beta_r^{-1}$. The related problem of a circular reinforcement bonded on a large (unholed) plate is briefly examined. This indicates how the normalisation stress for *SCF* relates to that applied beyond the patch.

The analytical formulae derived here provide convenient estimates for design purposes.

Authors

C. Pickthall.
Airframes and Engines Division

Colin Pickthall completed a B. Sc. (Hons.) in Physics at Monash University in 1985, and completed his Ph.D. at Monash University in 1993.

He commenced work in Materials Division at the (then named) Aeronautical Research Laboratory in 1991. His work has focussed on theoretical and analytical approaches in the areas of stress analysis and fracture mechanics, together with some finite element validation. He is currently a Research Scientist in the Airframes and Engines Division.

L.R.F. Rose
Airframes and Engines Division

Francis Rose graduated with a B.Sc (Hons) from Sydney University in 1971 and a PhD from Sheffield University, UK in 1975.
He was appointed as a Research Scientist at the Aeronautical Research Laboratory in 1976 and is currently the Research Leader in Fracture Mechanics in the Airframes and Engines Division.
He has made important research contributions in fracture mechanics, non-destructive evaluation and applied mathematics. He is the regional Editor for the International Journal of Fracture and a member of the editorial board of Mechanics of Materials. He is also a Fellow of the Institute for Applied Mathematics and its Applications, UK and a Fellow of the Institution of Engineers, Australia.

Contents

1. Introduction

A common problem is that of repairing a plate which has a hole in it, either deliberately inserted during construction or for internal access, or caused by accident. The deliberately inserted holes are often circular. Accidental holes may be irregularly shaped and have tears extending from them, but as part of the repair process, the damage is frequently cut out in a smooth, approximately circular shape. This removes cracks and stress concentrations at sharp corners of the initial damage. The next step is to place a reinforcement patch over the damage to exclude the environment, and reduce the (tangential hoop) stresses at the hole edges to below a maximum safe level. The patch may be rivetted, bolted or adhesively bonded. In this work, it is bonded. A thin layer of adhesive, principally through shear, transfers load between the reinforcement (patch) and the plate over a characteristic (load transfer) length. If the hole is much smaller than this length, then little load can be transferred to the reinforcement, and the tangential stress, $\sigma_{\theta\theta}$ at the hole boundary approaches twice the far field value in the plate under the reinforcement. For uniaxial loading, this factor is three times.

In this work, the situation is idealised as a circular hole in an infinite plate, with identical adhesively bonded reinforcement patches on both sides so that bending effects can be ignored. In general, the remote loading is biaxial where the orthogonal (longitudinal) stresses need not be equal. Any remote shear stresses can be eliminated by rotating coordinates. The analysis of this problem is simplified considerably if the remote loading is axi-symmetric (independent of angle) and purely radial. This is equivalent to equal biaxial loading (fig. 1) wherein $\sigma_{xx}=\sigma_{yy}=\sigma$ ($=\sigma_{rr}$), but is not truly hydrostatic as there is no stress applied in the third direction: $\sigma_{zz}=0$. Such axial symmetry reduces the problem to one-dimensional in the radial coordinate, and eliminates tangential displacements. As indicated later, it is possible to have axial symmetry but with non-zero tangential displacements.

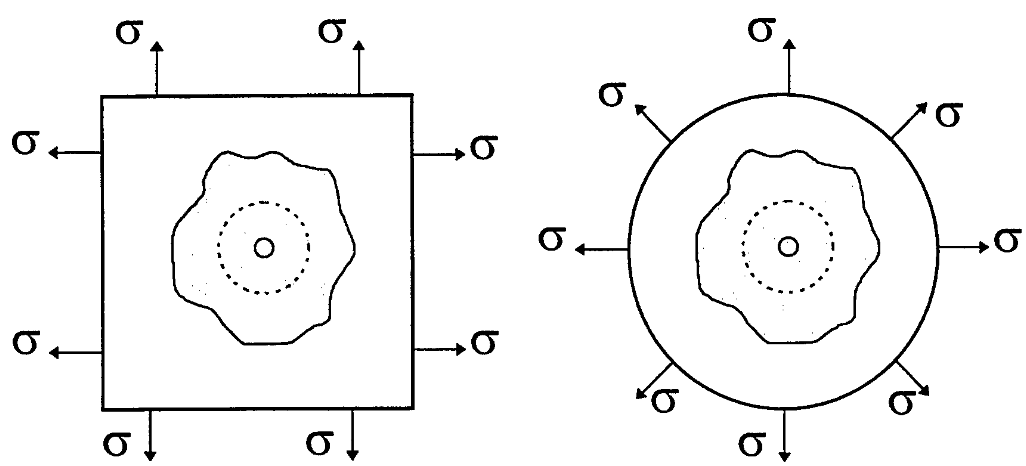

Figure 1. Equivalence of equal biaxial and axi-symmetric radial remote loading.

The analysis is taken as far as possible in the general case before several approximations including the radial loading, are discussed. The displacements in the plate and reinforcement are the functions to be found. Plane stress is assumed in the elasticity formulae. This is because the underlying problem is the patching of thin plates with no stresses applied normal to the surface: a quasi 2-dimensional problem.
The physical problem is shown in fig. 2. The plate is assumed very large, and the loads applied to its edges. The patch is also assumed large compared to the hole (of radius R), so that between the hole and the patch boundary, and far from each (shown dotted), there is a region of uniform and equal strain in the plate and reinforcement. The notion of "far" in practical terms means at least 3-4 load transfer lengths.

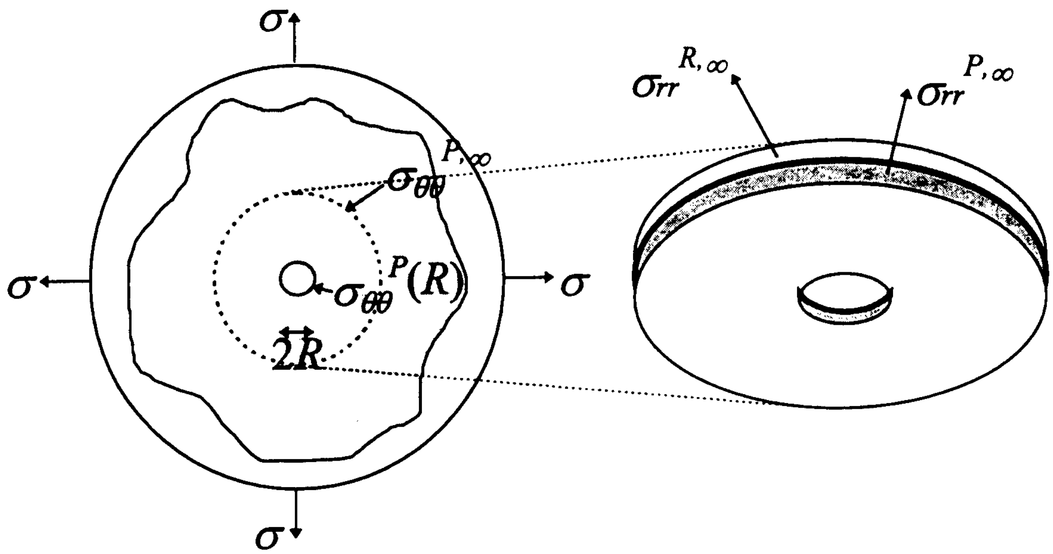

Figure 2. The problem examined is extracted from a larger physical situation.

The stress concentration factor (SCF) around the hole is defined as the stress at the boundary, $\sigma_{\theta\theta}^{P}(R)$ divided by that in the plate under this uniform strain region, $\sigma_{\theta\theta}^{P,\infty}$. This has an advantage over dividing by the stress in the plate outside the reinforcement (σ): it eliminates a geometrical dependence in the small hole limit when the reinforcement becomes ineffective, and as indicated earlier the SCF approaches two. Here, the interest is in how the reinforcement effectiveness depends on hole size. In a practical situation, the stress reduction in the plate under the reinforcement ($\sigma_{\theta\theta}^{P,\infty}$ compared to σ) would also be important. Further, the modification to the stress distribution in the whole structure due the additional stiffness of the reinforcement would have to be considered.

2. Formulation of the equations of equilibrium

In the plate and reinforcement, only in-plane stresses are considered. The adhesive is assumed to transfer load from the plate to the reinforcement through shear only. Peel and longitudinal stresses in the adhesive are neglected. The following figure shows the coordinate system and the stresses considered in the plate.

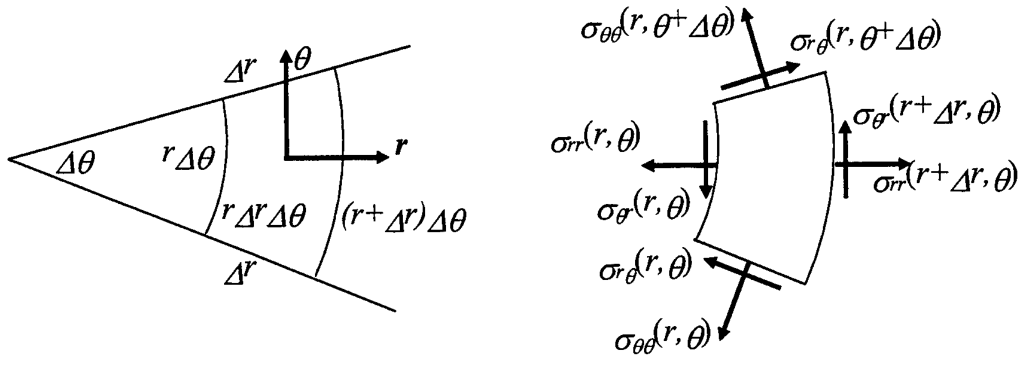

Figure 3. The infinitesimal element and forces considered.

From these figures, equations of equilibrium for annular segments of the plate and reinforcement, are obtained. The forces are obtained by multiplying the applicable stresses by the areas over which they act, and taking into account the components of the resulting forces in the directions being considered. To derive these equations, a section through the plate and reinforcement (fig. 4) is considered. It demonstrates how the adhesive transfers the loads, and the definition of the displacements.

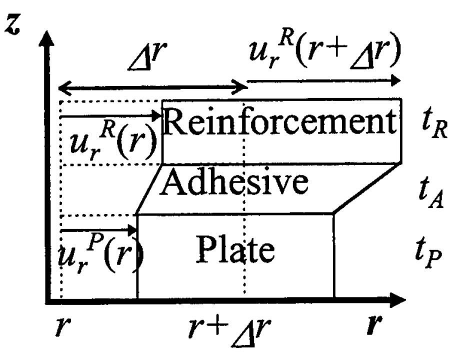

Figure 4. Section through the problem. The adhesive transfers load to the reinforcement through shear.

The forces exerted on the plate by the adhesive are given by:

Radial: $F_r^A = 2\mu_A e_{rz}^A \times r\Delta r\Delta\theta$ with the strains given by $2e_{rz}^A = \left(u_r^R - u_r^P\right)/t_A$.(1)

Tangential: $F_\theta^A = 2\mu_A e_{\theta z}^A \times r\Delta r\Delta\theta$ $\quad 2e_{\theta z}^A = \left(u_\theta^R - u_\theta^P\right)/t_A$

The opposites of these forces are exerted on the reinforcement.

Considering the radial and tangential equilibrium conditions for the plate and reinforcement respectively, noting that rotational equilibrium merely yields $\sigma_{r\theta}=\sigma_{\theta r}$ in both cases, the following equations result.

Reinforcement:

$$\text{Radial:}\quad \frac{\partial}{\partial r}\sigma_{rr}^R + \frac{1}{r}\frac{\partial}{\partial\theta}\sigma_{r\theta}^R + \frac{1}{r}\left(\sigma_{rr}^R - \sigma_{\theta\theta}^R\right) = \frac{\mu_A}{t_A t_R}\left(u_r^R - u_r^P\right)$$

$$\text{Tangential:}\quad \frac{1}{r}\frac{\partial}{\partial\theta}\sigma_{\theta\theta}^R + \frac{\partial}{\partial r}\sigma_{\theta r}^R + \frac{2\sigma_{\theta r}^R}{r} = \frac{\mu_A}{t_A t_R}\left(u_\theta^R - u_\theta^P\right) \qquad (2a)$$

Plate:

$$\text{Radial:}\quad \frac{\partial}{\partial r}\sigma_{rr}^{P}+\frac{1}{r}\frac{\partial}{\partial\theta}\sigma_{r\theta}^{P}+\frac{1}{r}\left(\sigma_{rr}^{P}-\sigma_{\theta\theta}^{P}\right)=\frac{-\mu_A}{t_A t_P}\left(u_r^R-u_r^P\right)$$
$$\text{Tangential:}\quad \frac{1}{r}\frac{\partial}{\partial\theta}\sigma_{\theta\theta}^{P}+\frac{\partial}{\partial r}\sigma_{\theta r}^{P}+\frac{2\sigma_{\theta r}^{P}}{r}=\frac{-\mu_A}{t_A t_P}\left(u_\theta^R-u_\theta^P\right) \qquad (2b)$$

The stresses above need to be expressed in terms of strains, assuming plane stress conditions, and then re-expressed in terms of the displacement functions. These are the functions which are then solved for. The equations needed are presented below.

2.1 Elasticity formulae

$$\begin{array}{lll} E=2\mu(1+\nu) & \text{plane stress:} & \text{plane strain:} \\ \sigma_{rr}+\sigma_{\theta\theta}=2\mu(2A+1)(e_{rr}+e_{\theta\theta}) & 2A+1=\dfrac{1+\nu}{1-\nu} & 2A+1=\dfrac{1}{1-2\nu}. \\ \sigma_{rr}-\sigma_{\theta\theta}=2\mu(e_{rr}-e_{\theta\theta}) & K=\dfrac{3-\nu}{1+\nu} & K=3-4\nu \end{array} \qquad (3)$$

The following formulae convert stresses to derivatives of displacement:

$$\begin{array}{ll} 2\sigma_{rr}=\dfrac{2E}{1-\nu^2}\left(e_{rr}+\nu e_{\theta\theta}\right) & e_{rr}=\dfrac{\partial u_r}{\partial r} \\ 2\sigma_{\theta\theta}=\dfrac{2E}{1-\nu^2}\left(\nu e_{rr}+e_{\theta\theta}\right) & e_{\theta\theta}=\dfrac{1}{r}\dfrac{\partial u_\theta}{\partial\theta}+\dfrac{1}{r}u_r \\ 2\sigma_{r\theta}=2\mu 2e_{r\theta} & 2e_{r\theta}=\dfrac{\partial u_\theta}{\partial r}+\dfrac{1}{r}\dfrac{\partial u_r}{\partial\theta}-\dfrac{1}{r}u_\theta \end{array} \qquad (4)$$

2.2 General formulae

Substituting the above into the equations of equilibrium produces the general equations for the displacements in the plate and reinforcement. They are long, and only the two for the reinforcement are presented below. The equations for the plate are obtained by interchanging "R" and "P", which also takes care of the reversal of the force exerted by the adhesive. For the reinforcement,

Radial:
$$\left[2\left(\frac{\partial^2}{\partial r^2}+\frac{1}{r}\frac{\partial}{\partial r}-\frac{1}{r^2}\right)+\frac{(1-\nu_R)}{r^2}\frac{\partial^2}{\partial\theta^2}\right]u_r^R+\left[\frac{(1+\nu_R)}{r}\frac{\partial^2}{\partial r\partial\theta}+\frac{(-3+\nu_R)}{r^2}\frac{\partial}{\partial\theta}\right]u_\theta^R=\frac{\mu_A}{t_A}\frac{(1-\nu_R)}{t_R\mu_R}\left(u_r^R-u_r^P\right)$$
Tangential:
$$\left[(1-\nu_R)\left(\frac{\partial^2}{\partial r^2}+\frac{1}{r}\frac{\partial}{\partial r}-\frac{1}{r^2}\right)+\frac{2}{r^2}\frac{\partial^2}{\partial\theta^2}\right]u_\theta^R+\left[\frac{(1+\nu_R)}{r}\frac{\partial^2}{\partial r\partial\theta}+\frac{(3-\nu_R)}{r^2}\frac{\partial}{\partial\theta}\right]u_r^R=\frac{\mu_A}{t_A}\frac{(1-\nu_R)}{t_R\mu_R}\left(u_\theta^R-u_\theta^P\right) \qquad . (5)$$

In these formulae, the arguments of the displacements, (r,θ), have been omitted for clarity.
A number of different (restrictive) assumptions facilitate solution of these equations under special circumstances.

3. Simplified cases

3.1 Single plate assumption

As a check on the above derivation, setting the adhesive force term (RHS) to zero, and then only taking the equations for the plate, gives the equations for the plate with a hole problem. Although already solved (appendix 1), this problem serves to illustrate the method of solving other problems reduced from the general case. It is also relevant for the region of the reinforcement over the hole in the plate. The full solution is split into angularly independent and angularly dependent parts.

Angularly independent solution
Firstly, if a solution independent of angle is assumed, then the replacements $\partial / \partial\theta \to 0$ and $\partial / \partial r \to \mathrm{d} / \mathrm{d}r$ can be made. This case may represent an annulus with distributed radial and tangential stresses applied on the inner and outer edges. In that case, both the radial and tangential equations reduce to:

$$\left(\frac{\mathrm{d}^2}{\mathrm{d}r^2}+\frac{1}{r}\frac{\mathrm{d}}{\mathrm{d}r}-\frac{1}{r^2}\right)h(r)=0, \qquad (6)$$

where $h(r)=u_\theta(r)$ or $u_r(r)$. If the solution is a power series in r, there is no mixing of terms with different powers, so the solution can be taken as a single term: $h(r)=B_m r^m$ and allowable values determined for m. This results in $(m^2\text{-}1)B_m=0$. Thus $m=\pm1$, $h(r)=B_{-1}/r+B_1 r$, and B_{-1} and B_1 will be chosen to match the boundary conditions.

Angularly dependent solution
Introducing angular dependence, the radial and tangential equations above respectively combine

$$\frac{1}{r^{2-k}}\left(\frac{\partial}{\partial r}\right)^k u_r, \frac{1}{r^2}\frac{\partial^2 u_r}{\partial\theta^2}, \frac{1}{r^{2-l}}\left(\frac{\partial}{\partial r}\right)^l \frac{\partial u_\theta}{\partial\theta} \text{ and } \frac{1}{r^{2-k}}\left(\frac{\partial}{\partial r}\right)^k u_\theta, \frac{1}{r^2}\frac{\partial^2 u_\theta}{\partial\theta^2}, \frac{1}{r^{2-l}}\left(\frac{\partial}{\partial r}\right)^l \frac{\partial u_r}{\partial\theta}.$$

Here k can be 0,1,2 and l 0,1, but all terms end up of order r^{-2} times their original power of r. Assuming the problem will be symmetric about the (suitably chosen) x and y axes, anticipating unequal perpendicularly applied uniaxial stresses parallel to the axes, then the solution must be of the form:

$$\begin{aligned} u_r(r,\theta) &= f(r)\cos(2n\theta) \\ u_\theta(r,\theta) &= g(r)\sin(2n\theta) \end{aligned}, \qquad (7)$$

n being an integer equal to 1 for the above anticipated loading case.
Once again, the radial parts of each function can be taken as single terms (of the same power, m) in power series expansions: $f(r)=C_m r^m$ and $g(r)=D_m r^m$. These forms result in the replacements $\frac{\partial}{\partial r}\to\frac{m}{r}, \frac{\partial^2}{\partial r^2}\to\frac{m(m-1)}{r^2}, \frac{\partial^2}{\partial\theta^2}\to -4$. Substitution into the radial and tangential equations, with these replacements, results in a pair of simultaneous equations for the coefficients C_m and D_m:

$$\begin{bmatrix} m^2+2\nu-3 & m(1+\nu)+\nu-3 \\ -2m(1+\nu)+2\nu-6 & m^2(1-\nu)+\nu-9 \end{bmatrix}\begin{bmatrix} C_m \\ D_m \end{bmatrix}=\begin{bmatrix} 0 \\ 0 \end{bmatrix}. \tag{8}$$

A non-trivial solution (C_m and D_m non-zero) requires the determinant to be zero: $(1-\nu)(m^2-1)(m^2-9)=0$. For each allowed value of m, a relationship then exists between C_m and D_m as indicated in the following table. The known values are for the biaxially loaded plate case shown in Appendix A.

Table 1. Relationships between coefficients, and values for the hole in a plate problem.

Value for m	Relationship	Known C_m	Known D_m
-1	$D_{-1}=-(1-\nu)C_{-1}/2$	$R^2(K+1)/2$	$R^2(-K+1)/2$
1	$D_1=-C_1$	1/2	-1/2
-3	$D_{-3}=C_{-3}$	$-R^4/2$	$-R^4/2$
3	$D_3=-(3+\nu)C_3/(2\nu)$	0	0

3.2 Equal Poisson's Ratios

This simplification is valid when the reinforcement is of the same material as the plate (same modulus as well), and may also be a good approximation if the two Poisson's ratios are similar. Indeed, for the representative bonded composite repair the Poisson's ratios are similar: 0.33 for aluminium and 0.30 for the reinforcement (Appendix 3). This simplification enables subtraction of the two radial and tangential equations respectively, to give equations for the relative displacements of the plate and reinforcement. Making the identifications $\Delta u_r = u_r^R - u_r^P$ and $\Delta u_\theta = u_\theta^R - u_\theta^P$, the resulting equations are:

Radial:

$$\left[2\left(\frac{\partial^2}{\partial r^2}+\frac{1}{r}\frac{\partial}{\partial r}-\frac{1}{r^2}\right)+\frac{(1-\nu)}{r^2}\frac{\partial^2}{\partial\theta^2}\right]\Delta u_r+\left[\frac{(1+\nu)}{r}\frac{\partial^2}{\partial r\partial\theta}+\frac{(-3+\nu)}{r^2}\frac{\partial}{\partial\theta}\right]\Delta u_\theta=\frac{\mu_A}{t_A}(1-\nu)\left(\frac{1}{t_R\mu_R}+\frac{1}{t_P\mu_P}\right)\Delta u_r\ . \tag{9}$$

Tangential:

$$\left[(1-\nu)\left(\frac{\partial^2}{\partial r^2}+\frac{1}{r}\frac{\partial}{\partial r}-\frac{1}{r^2}\right)+\frac{2}{r^2}\frac{\partial^2}{\partial\theta^2}\right]\Delta u_\theta^R+\left[\frac{(1+\nu)}{r}\frac{\partial^2}{\partial r\partial\theta}+\frac{(3-\nu)}{r^2}\frac{\partial}{\partial\theta}\right]\Delta u_r=\frac{\mu_A}{t_A}(1-\nu)\left(\frac{1}{t_R\mu_R}+\frac{1}{t_P\mu_P}\right)\Delta u_\theta$$

This case was not pursued any further: after solving the above coupled equations for the relative displacements Δu_r and Δu_θ, these solutions would be substituted back and the equations (5) solved for the actual displacements.

3.3 Angularly independent assumption

It is important to point out that there is a difference between assuming angular independence and zero angular displacement. The former allows both radial and tangential displacement as long as neither depends on the angle. In this case, the remote loadings on the plate and reinforcement, and on the surface of the hole in the plate, are independent of angle. They may be equal perpendicular remote uniaxial loads ("hydrostatic" loading $\sigma_{xx}^\infty=\sigma_{yy}^\infty$ but $\sigma_{zz}^\infty=0$), coupled with a pressure on the surface of the hole in the plate. Another situation could be different tangential loads applied to the hole surface and plate and reinforcement far from the hole, in a twisting

mode. The only requirement is that the loading be independent of angle. The more restrictive zero angular displacement situation limits all forces to the radial direction. Under the angular independence assumption, $\partial/\partial\theta \to 0$ and $\partial/\partial r \to \mathrm{d}/\mathrm{d}r$ as indicated earlier for the single plate case. This greatly simplifies the equations to be solved as shown.

$$\begin{array}{lll}
\text{Radial:} & \text{Reinforcement:} & 2\left(\dfrac{\mathrm{d}^2}{\mathrm{d}r^2}+\dfrac{1}{r}\dfrac{\mathrm{d}}{\mathrm{d}r}-\dfrac{1}{r^2}\right)u_r^R = \dfrac{\mu_A}{t_A}g_R\left(u_r^R-u_r^P\right) \\
 & \text{Plate:} & 2\left(\dfrac{\mathrm{d}^2}{\mathrm{d}r^2}+\dfrac{1}{r}\dfrac{\mathrm{d}}{\mathrm{d}r}-\dfrac{1}{r^2}\right)u_r^P = -\dfrac{\mu_A}{t_A}g_P\left(u_r^R-u_r^P\right) \\
\text{Tangential:} & \text{Reinforcement:} & \left(\dfrac{\mathrm{d}^2}{\mathrm{d}r^2}+\dfrac{1}{r}\dfrac{\mathrm{d}}{\mathrm{d}r}-\dfrac{1}{r^2}\right)u_\theta^R = \dfrac{\mu_A}{t_A}\dfrac{1}{t_R\mu_R}\left(u_\theta^R-u_\theta^P\right) \\
 & \text{Plate:} & \left(\dfrac{\mathrm{d}^2}{\mathrm{d}r^2}+\dfrac{1}{r}\dfrac{\mathrm{d}}{\mathrm{d}r}-\dfrac{1}{r^2}\right)u_\theta^P = -\dfrac{\mu_A}{t_A}\dfrac{1}{t_P\mu_P}\left(u_\theta^R-u_\theta^P\right)
\end{array} \tag{10}$$

where $g_R = \dfrac{(1-\nu_R)}{t_R\mu_R} = \dfrac{2(1-\nu_R^2)}{E_R t_R}$ and $g_P = \dfrac{(1-\nu_P)}{t_P\mu_P} = \dfrac{2(1-\nu_P^2)}{E_P t_P}$.

Subtracting the second radial equation from the first produces a single equation for the relative displacement, defined as for the equal Poisson's ratio case. This can also be done for the two tangential equations.

$$\begin{array}{lll}
\text{Radial:} & \left(\dfrac{\mathrm{d}^2}{\mathrm{d}r^2}+\dfrac{1}{r}\dfrac{\mathrm{d}}{\mathrm{d}r}-\dfrac{1}{r^2}\right)\Delta u_r = \beta_r^2\Delta u_r & \beta_r^2 = \dfrac{\mu_A}{2t_A}\left(g_R+g_P\right) \\
\text{Tangential:} & \left(\dfrac{\mathrm{d}^2}{\mathrm{d}r^2}+\dfrac{1}{r}\dfrac{\mathrm{d}}{\mathrm{d}r}-\dfrac{1}{r^2}\right)\Delta u_\theta = \beta_\theta^2\Delta u_\theta & \beta_\theta^2 = \dfrac{\mu_A}{t_A}\left(\dfrac{1}{t_R\mu_R}+\dfrac{1}{t_P\mu_P}\right)
\end{array} . \tag{11}$$

These equations have the same form, and after substituting $s=\beta_r r$ or $s=\beta_\theta r$, are identical to the modified Bessel equation (described in appendix 2) with order n=1. Different boundary conditions will lead to differences in their complete solutions.

The focus now will be on the radial displacements rather than tangential. The remote loading will be assumed purely radial in nature and the tangential displacements therefore $\Delta u_\theta(r)$=0. In this case, the solution for the relative radial displacement is $\Delta u(r) = AI_1(s) + BK_1(s)$ with $s=\beta_r r$. The solution must not diverge faster than O(s) as $s\to\infty$, therefore A=0.

Returning to the equations (10) for the radial displacements for the plate and reinforcement, they become

$$\begin{array}{ll}
\text{Reinforcement:} & \\
\left(\dfrac{\mathrm{d}^2}{\mathrm{d}s^2}+\dfrac{1}{s}\dfrac{\mathrm{d}}{\mathrm{d}s}-\dfrac{1}{s^2}\right)u_r^R(s) = \gamma_R BK_1(s) & \gamma_R = \dfrac{\mu_A}{2t_A}\dfrac{1}{\beta_r^2}g_R = \dfrac{g_R}{g_R+g_P} \\
\text{Plate:} & \\
\left(\dfrac{\mathrm{d}^2}{\mathrm{d}s^2}+\dfrac{1}{s}\dfrac{\mathrm{d}}{\mathrm{d}s}-\dfrac{1}{s^2}\right)u_r^P(s) = -\gamma_P BK_1(s) & \gamma_P = \dfrac{\mu_A}{2t_A}\dfrac{1}{\beta_r^2}g_P = \dfrac{g_P}{g_R+g_P}
\end{array} . \tag{12}$$

Focussing on the reinforcement equation, it will have complementary and particular solutions. The complementary solution is obtained on setting B=0. This was solved earlier for the single plate problem, and results in $u_r^{R,\mathrm{Comp}}(s) = C_1^R s + C_{-1}^R / s$ with the arbitrary constants $C_1{}^R$ and $C_{-1}{}^R$ to be determined by the boundary conditions.
The particular solution may be defined as $u_r{}^{R,\mathrm{Part}}(s)=\gamma_R BP(s)$.This results in the modified Bessel equation of order n=1 and thus $P(s)=K_1(s)$. Similar reasoning applies for the plate equation. Outside the hole ($r>R$, scaled radius $s>s_R=\beta_r R$), the overall solution is then:

$$\begin{aligned} u_r^R(s>s_R) &= C_1^R s + C_{-1}^R / s + \gamma_R B K_1(s) \\ u_r^P(s>s_R) &= C_1^R s + C_{-1}^R / s - \gamma_P B K_1(s) \end{aligned} \qquad (13)$$

Inside the hole, the reinforcement has the same equation and general form solution as the single plate as there is no adhesive force there. That is

$$\begin{aligned} &\left(\frac{\mathrm{d}^2}{\mathrm{d}s^2} + \frac{1}{s}\frac{\mathrm{d}}{\mathrm{d}s} - \frac{1}{s^2}\right) u_r^{R,-}(s) = 0 \\ &u_r^{R,-}(s<s_R) = D_1^R s + D_{-1}^R / s \end{aligned} \qquad (14)$$

As the solution must be regular at the origin, $D_{-1}{}^R=0$.

3.4 Boundary conditions

There are four boundary conditions, used to determine the four non-zero arbitrary constants B, $C_{-1}{}^R$, $C_1{}^R$ and $D_{-1}{}^R$. These are summarised below and then each interpreted in terms of the arbitrary constants.

$$\begin{array}{ll} \text{Continuity of displacements:} & u_r^R(s \to s_R^-) = u_r^R(s \to s_R^+) \\ \text{Continuity of radial stress:} & \sigma_{rr}^R(s \to s_R^-) = \sigma_{rr}^R(s \to s_R^+) \\ \text{Stress free hole surface:} & \sigma_{rr}^P(s \to s_R^+) \to 0 \\ \text{Far field radial loading:} & \begin{cases} \sigma_{rr}^R(s \to \infty) \to \sigma_{rr}^{R,\infty} \\ \sigma_{rr}^P(s \to \infty) \to \sigma_{rr}^{P,\infty} \end{cases} \end{array} \qquad (15)$$

There is also a relationship between the far field loading stresses on the plate and reinforcement, necessitated by the earlier solution where $\Delta u_r \to 0$ as $s \to \infty$.
The first boundary condition gives the first equation relating the arbitrary constants:

$$D_1^R s_R = C_1^R s_R + C_{-1}^R / s_R + \gamma_R B K_1(s_R). \qquad (16)$$

The other three boundary conditions require relationships for stresses in terms of the displacements. From the elasticity equations (4) presented earlier, and assuming $\partial/\partial\theta \to 0$, for both the plate and reinforcement (dropping the distinguishing "R" or "P" labels),

$$\begin{aligned} 2\sigma_{rr}(r) &= \frac{2\times 2\mu}{1-\nu}\left(\frac{\mathrm{d}}{\mathrm{d}r} + \frac{\nu}{r}\right) u_r(r) = \frac{4\mu}{1-\nu}\beta_r\left(\frac{\mathrm{d}}{\mathrm{d}s} + \frac{\nu}{s}\right) u_r(s) \\ 2\sigma_{\theta\theta}(r) &= \frac{4\mu}{1-\nu}\beta_r\left(\nu\frac{\mathrm{d}}{\mathrm{d}s} + \frac{1}{s}\right) u_r(s) \end{aligned} \qquad (17)$$

The second and third boundary conditions then become, after using the Bessel function relationships in appendix 2 to evaluate the derivatives,

$$
\begin{aligned}
D_1^R\left(1+\nu_R\right) &= C_1^R\left(1+\nu_R\right)+C_{-1}^R\frac{\left(-1+\nu_R\right)}{s_R^2}+\gamma_R B\left[-K_0(s_R)+\frac{\left(-1+\nu_R\right)}{s_R}K_1(s_R)\right] \\
0 &= C_1^R\left(1+\nu_P\right)+C_{-1}^R\frac{\left(-1+\nu_P\right)}{s_R^2}-\gamma_P B\left[-K_0(s_R)+\frac{\left(-1+\nu_P\right)}{s_R}K_1(s_R)\right]
\end{aligned}. \tag{18a}
$$

Turning to the fourth boundary condition, that relating to the far field loading, then in the limiting case as $r\to\infty$, or in scaled form $s\to\infty$, the equations become

$$
\begin{aligned}
&2\sigma_{rr}^R(s\to\infty)\to\frac{4\mu_R}{1-\nu_R}\beta_r\left(1+\nu_R\right)\,C_1^R+O(1/s^2)\to 2\sigma_{rr}^{R,\infty} \\
&2\sigma_{rr}^P(s\to\infty)\to\frac{4\mu_P}{1-\nu_P}\beta_r\left(1+\nu_P\right)\,C_1^R+O(1/s^2)\to 2\sigma_{rr}^{P,\infty}
\end{aligned}. \tag{18b}
$$

These two equations give C_1^R directly, as well as the relationship between the far field load on the plate and reinforcement needed to give $\Delta u_r(s\to\infty)\to 0$. This relationship is best expressed as

$$
\sigma_{rr}^{R,\infty}=\left(\frac{1+\nu_R}{1-\nu_R}\right)\left(\frac{1-\nu_P}{1+\nu_P}\right)\frac{\mu_R}{\mu_P}\sigma_{rr}^{P,\infty}=\frac{E_R\left(1-\nu_P\right)}{E_P\left(1-\nu_R\right)}\sigma_{rr}^{P,\infty}. \tag{19}
$$

The shear moduli have been expressed in terms of the (more commonly presented) Young's moduli in this equation. The ratio of tangential (hoop) stress at the hole surface to that far away in the plate, later referred to as the stress concentration factor $SCF=\sigma_{\theta\theta}^P(r=R)/\sigma_{\theta\theta}^{P,\infty}$, is of interest. Note that $\sigma_{\theta\theta}^{P,\infty}=\sigma_{rr}^{P,\infty}$ as the loading is axi-symmetric.

3.5 Solving for the arbitrary constants

In order to examine the weak/thick ($\beta_r\to 0$) and stiff/thin ($\beta_r\to\infty$) adhesive limits, the equations for the constants (16 and 18) must be rewritten by scaling the constants. The resulting matrix equation is:

$$
\begin{bmatrix} -\left(\beta_r C_1^R\right) \\ -\left(\beta_r C_1^R\right) \\ -\left(\beta_r C_1^R\right) \end{bmatrix}
=
\begin{bmatrix}
-1 & \dfrac{1}{R^2} & \gamma_R\beta_r^2\dfrac{K_1(s_R)}{s_R} \\
-1 & \dfrac{1}{R^2}\left(\dfrac{-1+\nu_R}{1+\nu_R}\right) & \gamma_R\beta_r^2\left(\dfrac{1}{1+\nu_R}\right)\left[-K_0(s_R)+\dfrac{\left(-1+\nu_R\right)}{s_R}K_1(s_R)\right] \\
0 & \dfrac{1}{R^2}\left(\dfrac{-1+\nu_P}{1+\nu_P}\right) & -\gamma_P\beta_r^2\left(\dfrac{1}{1+\nu_P}\right)\left[-K_0(s_R)+\dfrac{\left(-1+\nu_P\right)}{s_R}K_1(s_R)\right]
\end{bmatrix}
\begin{bmatrix} \left(\beta_r D_1^R\right) \\ \left(\dfrac{1}{\beta_r}D_1^R\right) \\ \left(\dfrac{1}{\beta_r}B\right) \end{bmatrix}. \tag{20}
$$

This set of equations simplifies in the small and large β_r limits, but can be solved directly before the limits are taken. Doing so leads to

$$
\begin{aligned}
\left(\beta_r C_1^R\right) &= \frac{\left(1-\nu_P\right)}{2\mu_P\left(1+\nu_P\right)}\sigma_{rr}^{P,\infty} \\
\left(\frac{1}{\beta_r}B\right) &= \frac{-2R^2\left(1+\nu_P\right)}{\left[\gamma_R\left(1-\nu_P\right)+2\gamma_P\right]s_R^2 K_0(s_R)+2\left(1-\nu_P\right)s_R K_1(s_R)}\left(\beta_r C_1^R\right) \\
\left(\frac{1}{\beta_r}C_{-1}^R\right) &= -\frac{\gamma_R}{2}\left[s_R^2 K_0(s_R)+2s_R K_1(s_R)\right]\left(\frac{1}{\beta_r}B\right) \\
\left(\beta_r D_1^R\right) &= -\frac{1}{2R^2\left(1+\nu_P\right)}\left[2s_R^2 K_0(s_R)+2\left(1-\nu_P\right)s_R K_1(s_R)\right]\left(\frac{1}{\beta_r}B\right)
\end{aligned}
\quad . \tag{21}
$$

These expressions now give the displacement functions analytically (equations 14 and 13), and from those, the radial and tangential stress fields can be obtained using equations (17).

The quantity of interest is the stress concentration factor *SCF* defined above. It requires the tangential stress in the plate. From equation (17),

$$
\sigma_{\theta\theta}^P(s) = \frac{2\mu_P}{\left(1-\nu_P\right)}\left\{\left(1+\nu_P\right)\left(\beta_r C_1^R\right)+\frac{\beta_r^2\left(1-\nu_P\right)}{s^2}\left(\frac{1}{\beta_r}C_{-1}^R\right)-\gamma_P\frac{\beta_r^2}{s}\left[-\nu_P s K_0(s)+\left(1-\nu_P\right)K_1(s)\right]\left(\frac{1}{\beta_r}B\right)\right\} . \tag{22}
$$

Substituting in the above expressions for the constants and $s=s_R$ at the hole surface, this simplifies down to

$$
\begin{aligned}
&\sigma_{\theta\theta}^P(s_R) = \sigma_{\theta\theta}^{P,\infty}\times SCF \quad \text{where} \quad SCF = \frac{2+F_K(s_R)}{1+hF_K(s_R)} \quad \text{and} \\
&F_K(s_R) = \frac{s_R K_0(s_R)}{K_1(s_R)} \quad \text{with} \quad h = \frac{2-\left(1+\nu_P\right)\gamma_R}{2\left(1-\nu_P\right)}
\end{aligned}
\quad . \tag{23}
$$

Here *SCF* is the stress concentration factor, which equals 2 for an unreinforced hole in an axi-symmetrically loaded plate, and 3 (Timoshenko[2]) if loaded uniaxially. The above expression is useful as all the geometric parameters concerning the components' thicknesses and moduli are included in the single parameter h. The hole radius enters in the scaled form $s_R=\beta_r R$. Parameters for a typical composite bonded repair of an aluminium plate are presented in appendix C. The behaviour of *SCF* with varying hole size for the typical reinforcement configuration, and where the reinforcement is the same aluminium as the plate, is shown below.

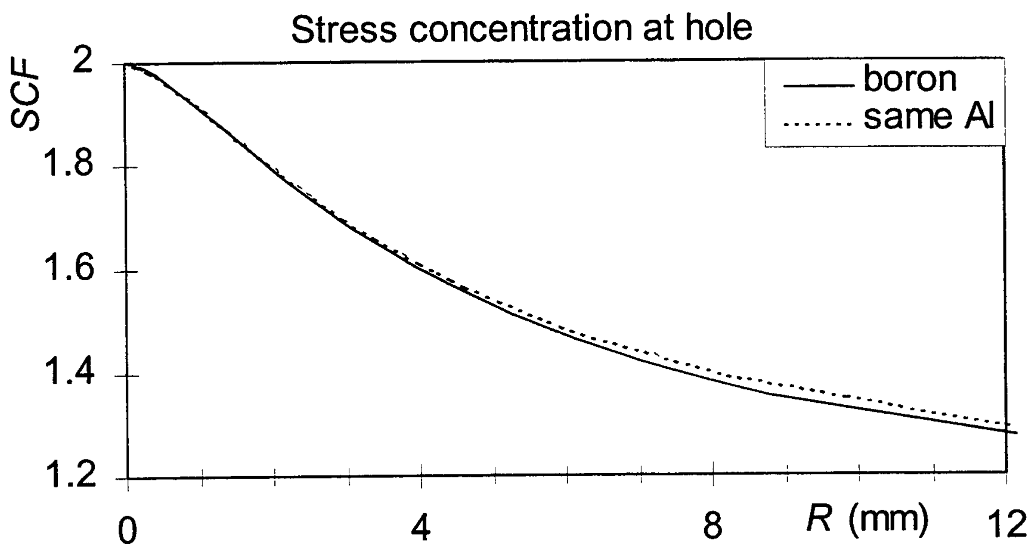

Figure 5. Stress concentration factor as a function of hole size for a representative geometry.

In normalised form, *SCF* against s_R for several values of *h*, is shown below.

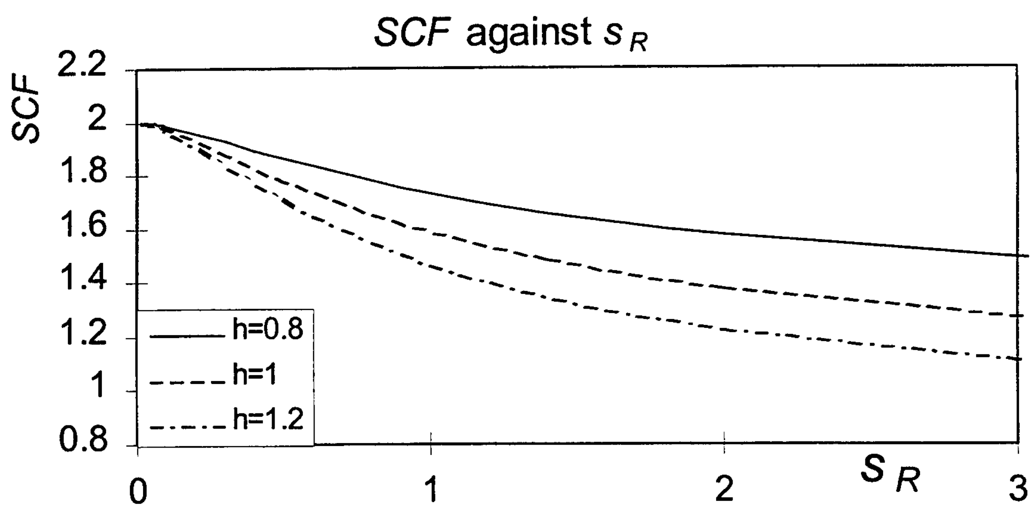

Figure 6. Stress concentration factor against hole size normalised by load transfer length.

3.6 Limiting values

The weak/thick and stiff/thin adhesive limiting values for *SCF* are useful because, with this work focussed on the effect of hole size, these limits are also the small and large hole limits respectively.

The limiting values are obtained from the Bessel function limiting expressions (appendix B) as:

$$
\begin{array}{lll}
\text{Weak adhesive, small hole:} & F_K(s_R \to 0) \to -(s_R^2)[\gamma + \ln(s_R/2)] + O(s_R^4)\ln(s_R/2) & \\
s_R = \beta_r R \to 0 & SCF(s_R \to 0) \to 2 - (1+2h)(s_R^2)[\gamma + \ln(s_R/2)] + O(s_R^4) & \\
\text{Strong adhesive, large hole:} & F_K(s_R \to \infty) \to s_R - 1/2 + O(1/s_R) & .\ (24) \\
s_R = \beta_r R \to \infty & SCF(s_R \to \infty) \to 1/h + \dfrac{2h-1}{h^2}\left(\dfrac{1}{s_R}\right) + O\left(\dfrac{1}{s_R^2}\right) &
\end{array}
$$

An interesting fact is that if the plate and reinforcement are identical ($\gamma_R=\gamma_P=1/2$), then the expression for h becomes $h=(3-\nu_P)/(4-4\nu_P)$. Poisson's ratio is usually close to 1/3, and if exactly that value, then h=1 precisely, and the large hole limit has $SCF\to 1$.

4. Plate with a finite reinforcement patch (no hole)

In the above derivations, the reinforcement was assumed infinitely large so that edge effects could be ignored and the "far field" remote loading produced a uniform radial strain. Here a finite circular reinforcement on an axi-symmetrically loaded plate is examined (fig. 7).

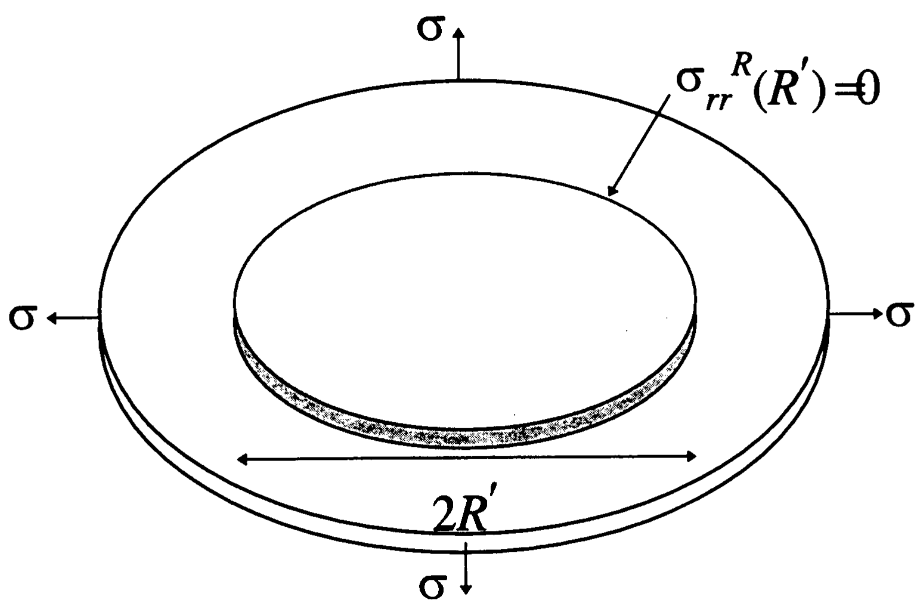

Figure 7 Finite reinforcement bonded on a large plate.

As before, the remote loading will be purely radial with zero tangential displacements. The solution for the relative radial displacement between the plate and reinforcement is: $\Delta u(r) = AI_1(s) + BK_1(s)$ with $s = \beta_r r$. This time, the solution must not diverge as $s\to 0$, therefore B=0. The equations for the radial displacements for the plate and reinforcement (equation 12), remain as before except that $BK_1(s)$ is replaced by $AI_1(s)$.

The complementary solution is the same: $u_r^{R,\mathrm{Comp}}(s) = E_1^R s + E_{-1}^R / s$ with the arbitrary constants renamed E_1^R and E_{-1}^R to distinguish them from the earlier constants. The particular solution may be defined as $u_r^{R,\mathrm{Part}}(s)=\gamma_R AP(s)$.This results in the modified Bessel equation of order n=1 and thus $P(s)=I_1(s)$. Similar reasoning applies for the plate

equation. Given that $I_1(s \to 0) \to 0$, E_{-1}^R must be zero as the displacements vanish at the centre. Inside the reinforcement radius ($r<R'$, scaled radius $s<s_{R'}=\beta_r R'$), the overall solution is then:

$$u_r^R(s<s_{R'}) = E_1^R s + \gamma_R A I_1(s)$$
$$u_r^P(s<s_{R'}) = E_1^R s - \gamma_P A I_1(s) \quad (25)$$

Outside the reinforcement, the plate satisfies the single plate equation (14) with general form solution:

$$u_r^{P,+}(s>s_{R'}) = F_1^P s + F_{-1}^P / s\,. \quad (26)$$

In this case, both terms are valid and hence retained.

4.1 Boundary conditions

There are four boundary conditions, used to determine the four non-zero arbitrary constants A, E_{-1}^R, F_1^P and F_{-1}^P. These are summarised below and then each interpreted in terms of the arbitrary constants.

$$\begin{array}{ll} \text{Continuity of plate displacements:} & u_r^P(s \to s_{R'}^+) = u_r^P(s \to s_{R'}^-) \\ \text{Continuity of radial plate stress:} & \sigma_{rr}^P(s \to s_{R'}^+) = \sigma_{rr}^P(s \to s_{R'}^-) \\ \text{Stress free reinforcement outer edge:} & \sigma_{rr}^R(s \to s_{R'}^-) \to 0 \\ \text{Far field plate loading:} & \sigma_{rr}^P(s \to \infty) \to \sigma \end{array} \quad (27)$$

The first boundary condition gives the first equation relating the arbitrary constants:

$$F_1^P s_{R'} + F_{-1}^P / s_{R'} = E_1^R s_{R'} - \gamma_P A I_1(s_{R'})\,. \quad (28a)$$

The second and third boundary conditions then become

$$0 = E_1^R(1+\nu_P) + \gamma_R A\left[I_0(s_{R'}) - \frac{(1-\nu_P)}{s_{R'}} I_1(s_{R'})\right]$$
$$F_1^P(1+\nu_P) + F_{-1}^P \frac{(-1+\nu_P)}{s_{R'}^2} = E_1^R(1+\nu_P) - \gamma_P A\left[I_0(s_{R'}) - \frac{(1-\nu_P)}{s_{R'}} I_1(s_{R'})\right] \quad (28b)$$

The fourth (far field) boundary condition, may be simplified as $s \to \infty$ by neglecting the F_{-1}^P term:

$$\sigma_{rr}^P(s \to \infty) \to \frac{2\mu_P}{1-\nu_P} \beta_r (1+\nu_P) F_1^P + O(1/s^2) \to \sigma\,. \quad (28c)$$

4.2 Solving for the arbitrary constants

Putting together the above equations, noting that the last gives F_1^P explicitly, the resulting matrix equation is:

$$\begin{bmatrix} (\beta_r F_1^P) \\ 0 \\ (\beta_r F_1^P) \end{bmatrix} = \begin{bmatrix} 1 & -\frac{1}{R'^2} & -\gamma_P \beta_r^2 \frac{I_1(s_{R'})}{s_{R'}} \\ -1 & 0 & \gamma_R \beta_r^2 \left(\frac{1}{1+\nu_R}\right)\left[I_0(s_{R'}) - \frac{(1-\nu_R)}{s_{R'}} I_1(s_{R'})\right] \\ 1 & \frac{1}{R'^2}\left(\frac{1-\nu_P}{1+\nu_P}\right) & -\gamma_P \beta_r^2 \left(\frac{1}{1+\nu_P}\right)\left[I_0(s_{R'}) - \frac{(1-\nu_P)}{s_{R'}} I_1(s_{R'})\right] \end{bmatrix} \begin{bmatrix} (\beta_r E_1^R) \\ \left(\frac{1}{\beta_r} F_{-1}^P\right) \\ \left(\frac{1}{\beta_r} A\right) \end{bmatrix}. \quad (29)$$

The solution, for all four constants, is

$$\begin{aligned}
\left(\beta_r F_1^P\right) &= \frac{(1-\nu_P)}{2\mu_P(1+\nu_P)}\sigma = \frac{(1-\nu_P)}{2E_P}\sigma \\
\left(\frac{1}{\beta_r}A\right) &= \frac{-2R'^2(1+\nu_R)}{\left[\gamma_P(1+\nu_R)+2\gamma_R\right]s_{R'}^2 I_0(s_{R'})-2(1-\nu_R)\gamma_R s_{R'} I_1(s_{R'})}\left(\beta_r F_1^P\right) \\
\left(\frac{1}{\beta_r}F_{-1}^P\right) &= \frac{\gamma_P}{2}\left[s_{R'}^2 I_0(s_{R'})-2s_{R'}I_1(s_{R'})\right]\left(\frac{1}{\beta_r}A\right) \\
\left(\beta_r E_1^R\right) &= \left(\beta_r F_1^P\right)+\frac{\gamma_P}{2R'^2}s_{R'}^2 I_0(s_{R'})\left(\frac{1}{\beta_r}A\right)
\end{aligned} \quad . \tag{30}$$

These expressions again give the displacement functions analytically (equations 25 and 26), and hence the radial and tangential stress fields. The stresses in the reinforcement and plate under the reinforcement are of interest, particularly far from the edge of the reinforcement and in the limit of a large reinforcement relative to the transfer length ($s_{R'}\to\infty$). Evaluation of this limit requires the large argument limits for the Bessel functions I_0, and I_1, equations 44. In this $s_{R'}\to\infty$ limit, the parameters become

$$\begin{aligned}
A &= \frac{-2\sqrt{2\pi}s_{R'}^{3/2}(1+\nu_R)\exp(-s_{R'})F_1^P}{s_{R'}\left[\gamma_P(1+\nu_R)+2\gamma_R\right]+\frac{1}{8}\left[1+\nu_R-15\gamma_R(1-\nu_R)\right]} \to -O\left(\sqrt{s_{R'}}\exp(-s_{R'})\right)F_1^P \\
F_{-1}^P &= \frac{-\gamma_P s_{R'}^2(1+\nu_R)\left(s_{R'}-\frac{15}{8}\right)F_1^P}{s_{R'}\left[\gamma_P(1+\nu_R)+2\gamma_R\right]+\frac{1}{8}\left[1+\nu_R-15\gamma_R(1-\nu_R)\right]} \approx \frac{-\gamma_P(1+\nu_R)s_{R'}^2 F_1^P}{\gamma_P(1+\nu_R)+2\gamma_R} \\
E_1^R &= F_1^P - \frac{\gamma_P(1+\nu_R)\left(s_{R'}+\frac{1}{8}\right)F_1^P}{s_{R'}\left[\gamma_P(1+\nu_R)+2\gamma_R\right]+\frac{1}{8}\left[1+\nu_R-15\gamma_R(1-\nu_R)\right]} \approx \frac{2\gamma_R F_1^P}{\gamma_P(1+\nu_R)+2\gamma_R}
\end{aligned} \quad . \tag{31}$$

In terms of the remote applied stress σ the stresses in the plate outside the reinforcement are

$$\begin{aligned}
\frac{\sigma_{rr}^P(s>s_{R'})}{\sigma} &= 1-\left(\frac{1-\nu_P}{1+\nu_P}\right)\left(\frac{F_{-1}^P}{F_1^P}\right)\frac{1}{s^2} \\
\frac{\sigma_{\theta\theta}^P(s>s_{R'})}{\sigma} &= 1+\left(\frac{1-\nu_P}{1+\nu_P}\right)\left(\frac{F_{-1}^P}{F_1^P}\right)\frac{1}{s^2}
\end{aligned} \quad . \tag{32}$$

Note that for the representative reinforcement parameters of appendix C, F_{-1}^P is negative. Inside R', the stresses are as follows.

$$
\begin{aligned}
\frac{\sigma_{rr}^{P}(s<s_{R'})}{\sigma} &= \frac{E_1^R}{F_1^P} - \frac{\gamma_P A}{(1+\nu_P)F_1^P}\left[I_0(s) - \frac{1-\nu_P}{s} I_1(s)\right] \\
\frac{\sigma_{\theta\theta}^{P}(s<s_{R'})}{\sigma} &= \frac{E_1^R}{F_1^P} - \frac{\gamma_P A}{(1+\nu_P)F_1^P}\left[\nu_P I_0(s) + \frac{1-\nu_P}{s} I_1(s)\right] \\
\frac{\sigma_{rr}^{R}(s<s_{R'})}{\sigma} &= \frac{\mu_R}{\mu_P}\frac{(1+\nu_R)}{(1-\nu_R)}\frac{(1-\nu_P)}{(1+\nu_P)}\left\{\frac{E_1^R}{F_1^P} + \frac{\gamma_R A}{(1+\nu_R)F_1^P}\left[I_0(s) - \frac{1-\nu_R}{s} I_1(s)\right]\right\} \\
\frac{\sigma_{\theta\theta}^{R}(s<s_{R'})}{\sigma} &= \frac{\mu_R}{\mu_P}\frac{(1+\nu_R)}{(1-\nu_R)}\frac{(1-\nu_P)}{(1+\nu_P)}\left\{\frac{E_1^R}{F_1^P} + \frac{\gamma_R A}{(1+\nu_R)F_1^P}\left[\nu_R I_0(s) + \frac{1-\nu_R}{s} I_1(s)\right]\right\}
\end{aligned}
\quad . \qquad (33)
$$

The values of these stresses as $s \rightarrow 0$ (centre of the reinforcement) are of interest. In the first two equations, the terms in square brackets (see equation 42) approach $(1+\nu_P)/2$, and the two stresses σ_{rr}^P and $\sigma_{\theta\theta}^P$ become equal. Similarly the stresses in the reinforcement also become equal. Hence

$$
\begin{aligned}
\frac{\sigma_{rr}^{P}(s\rightarrow 0)}{\sigma} &\rightarrow \frac{\sigma_{\theta\theta}^{P}(s\rightarrow 0)}{\sigma} \rightarrow \frac{2E_1^R - \gamma_P A}{2F_1^P} + O(s)^2 \\
\frac{\sigma_{rr}^{R}(s\rightarrow 0)}{\sigma} &\rightarrow \frac{\sigma_{\theta\theta}^{R}(s\rightarrow 0)}{\sigma} \rightarrow \frac{\mu_R}{\mu_P}\frac{(1+\nu_R)}{(1-\nu_R)}\frac{(1-\nu_P)}{(1+\nu_P)}\left\{\frac{2E_1^R + \gamma_R A}{2F_1^P}\right\} + O(s)^2
\end{aligned}
\quad . \qquad (34)
$$

Once again the large reinforcement limit is of interest as it represents the assumption made for the patched hole case examined earlier. In this case, the A terms vanish and the stress in the plate under the reinforcement becomes

$$
\left.\frac{\sigma_{rr}^{P}(s\rightarrow 0)}{\sigma}\right|_{s_{R'}\rightarrow\infty} \rightarrow \frac{E_1^R}{F_1^P} \rightarrow \frac{2\gamma_R}{\gamma_P(1+\nu_R)+2\gamma_R} . \qquad (35)
$$

This equation relates the loading assumed for the hole case (and thus the stress value $\sigma_{rr}^{P,\infty}$ of equations 15 and 19 used to normalise the stresses) to that in the plate beyond the reinforcement.

The displacements and stresses (latter normalised by the remote applied load σ) are plotted below for the representative bonded reinforcement.

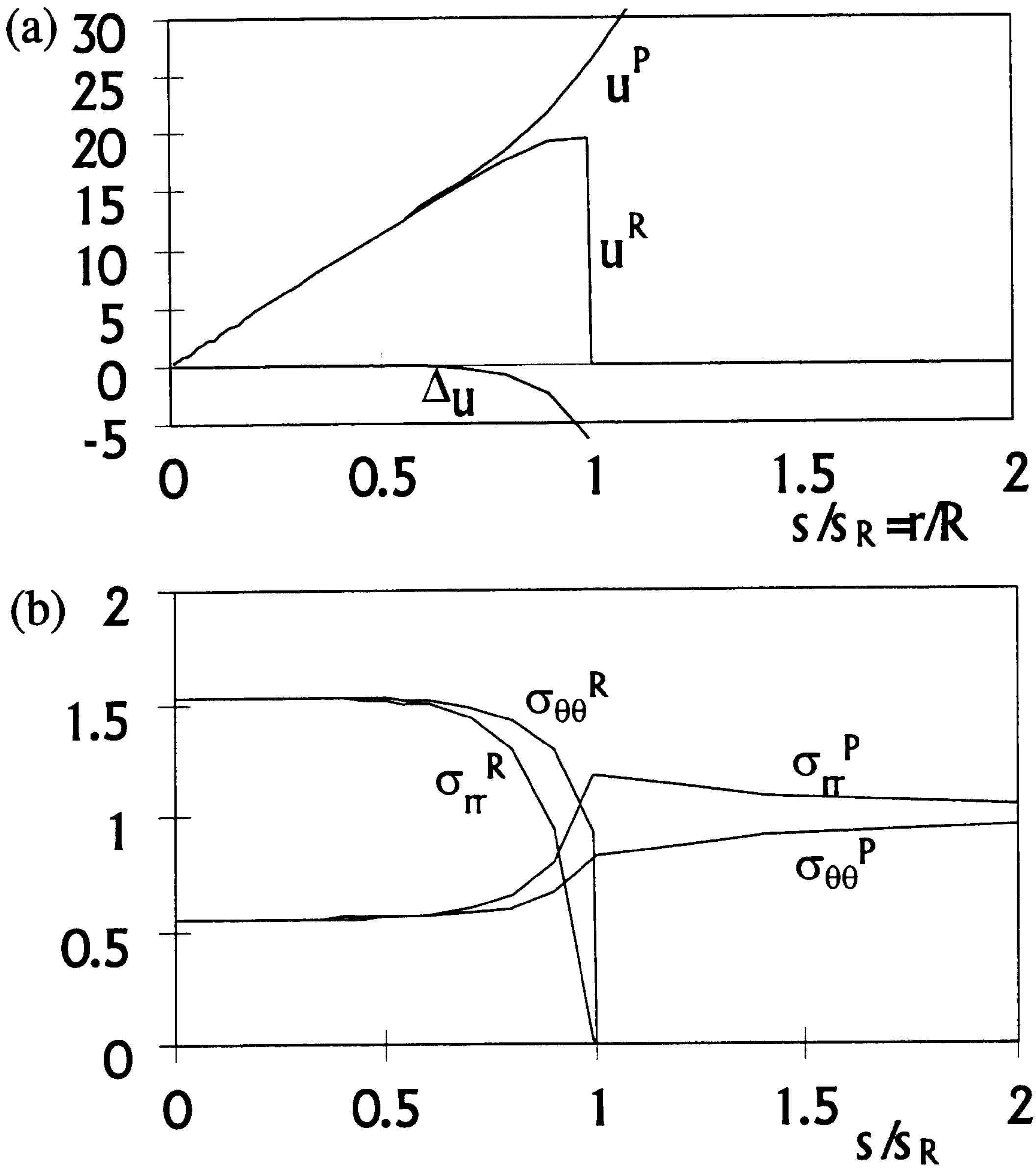

Figure 8 Plots of (a) the displacements and (b) stresses (normalised by the applied stress σ) for a circular reinforcement bonded onto a large plate.

5. Conclusions

The (two dimensional) equations for stresses and displacements for an infinite plate with a circular hole and (infinite) bonded reinforcement, are solved analytically for the case of axi-symmetric loading of the plate and reinforcement with vanishing adhesive shear stress at infinity. The conjugate problem of a finite circular reinforcement bonded on an infinite plate is also solved. It is useful in relating the stress in the plate under the

reinforcement in the first problem to the load applied beyond the reinforcement for a finite reinforcement over a hole. In solving these problems, two load transfer lengths are identified: one associated with radial displacements (β_r^{-1}) and the other tangential (β_θ^{-1}). The earlier solution leads to an analytical formula for the stress concentration factor (*SCF*): the ratio of the hoop stress at the surface of the hole relative to the far field plate loading. This formula incorporates all the geometrical parameters in a single non-dimensional parameter h. For a typical repair geometry, $h \approx 1$. The *SCF* is two in the absence of a reinforcement and in the limit of a small lole, but decreases as the hole size becomes a significant fraction of the load transfer length, approaching $1/h$ in the large hole limit. For a typical repair geometry, *SCF* has fallen to 1.6 by the time the hole size is equal to β_r^{-1} and 1.3 by $3\beta_r^{-1}$

6. References

1. LIST, R. D., "A Two-dimensional Circular Inclusion Problem", *Proc. Camb. Phil. Soc.*, **65**, 823-30, 1969.
2. TIMOSHENKO, S. P., and GOODIER, J. N. "Theory of Elasticity Third Edition", 1970, McGraw-Hill Book Company, New York.
3. ABRAMOWITZ, M. and STEGUN, I. A., "Handbook of Mathematical Functions with Formulas, Graphs, and Mathematical Tables", 1964, Nbs, Washington.
4. MUSKHELISHVILI, N. I., "Some Basic Problems of the Mathematical Theory of Elasticity", 1953, Noordhoff, Groningen, Holland.

1. Appendix A: Known solutions for biaxially loaded (single) plate with a hole.

The solution for an infinitely large plate remotely loaded with unequal perpendicular uniaxial stresses and a hole of radius R, is known (Timoshenko[2], Muskhelishvili[4], List[1]) analytically.

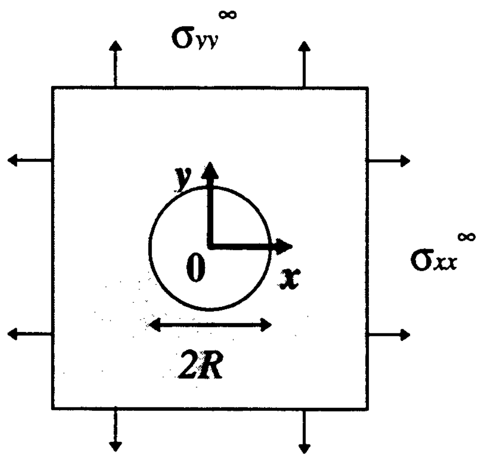

Figure 9 Biaxially loaded (unpatched) plate with a circular hole.

The radial and tangential equilibrium equations (reduced from equations 5) couple the radial (u_r) and tangential (u_θ) displacements:

$$
\begin{aligned}
&\text{Radial:}\\
&\left[2\left(\frac{\partial^2}{\partial r^2}+\frac{1}{r}\frac{\partial}{\partial r}-\frac{1}{r^2}\right)+\frac{(1-\nu)}{r^2}\frac{\partial^2}{\partial\theta^2}\right]u_r+\left[\frac{(1+\nu)}{r}\frac{\partial^2}{\partial r\partial\theta}+\frac{(-3+\nu)}{r^2}\frac{\partial}{\partial\theta}\right]u_\theta=0\\
&\text{Tangential:}\\
&\left[(1-\nu)\left(\frac{\partial^2}{\partial r^2}+\frac{1}{r}\frac{\partial}{\partial r}-\frac{1}{r^2}\right)+\frac{2}{r^2}\frac{\partial^2}{\partial\theta^2}\right]u_\theta+\left[\frac{(1+\nu)}{r}\frac{\partial^2}{\partial r\partial\theta}+\frac{(3-\nu)}{r^2}\frac{\partial}{\partial\theta}\right]u_r=0
\end{aligned}
\quad . \qquad (36)
$$

Using the functional forms of this paper, the solution separates into angularly independent and angularly dependent parts. With the boundary conditions of a (radial) stress free hole surface, and far field loading as described, the solution is:

$$
\begin{aligned}
u_r(r,\theta)&=h(r)+f(r)\cos(2\theta) & h(r)&=\frac{\sigma_h^\infty}{2\mu}\left[\left(\frac{R^2}{2}\right)\frac{1}{r}+\left(\frac{K-1}{4}\right)r\right]\\
& & f(r)&=\frac{\sigma_d^\infty}{2\mu}\left[\left(\frac{R^2(K+1)}{2}\right)\frac{1}{r}+\left(\frac{1}{2}\right)r-\left(\frac{R^4}{2}\right)\frac{1}{r^3}\right] \quad .(37)\\
u_\theta(r,\theta)&=g(r)\sin(2\theta) & g(r)&=\frac{\sigma_d^\infty}{2\mu}\left[\left(\frac{R^2(-K+1)}{2}\right)\frac{1}{r}-\left(\frac{1}{2}\right)r-\left(\frac{R^4}{2}\right)\frac{1}{r^3}\right]
\end{aligned}
$$

The stresses and K value (for plane stress) are given by:

$$\begin{array}{lll} \sigma_h^\infty = \sigma_{xx}^\infty + \sigma_{yy}^\infty & \sigma_d^\infty = \sigma_{xx}^\infty - \sigma_{yy}^\infty & \sigma_{xy}^\infty = 0 \\ K = \dfrac{3-\nu}{1+\nu} & K-1 = \dfrac{2(1-\nu)}{1+\nu} & K+1 = \dfrac{4}{1+\nu}. \end{array} \tag{38}$$

2. Appendix B: Modified Bessel Functions

The following information, from Abramowitz and Stegun [3], is provided for completeness.

2.1 Modified Bessel Equation:

$$\begin{aligned} & s^2\frac{\mathrm{d}^2F}{\mathrm{d}s^2} + s\frac{\mathrm{d}F}{\mathrm{d}s} - \left(s^2+n^2\right)F(s) = 0, \quad \text{or} \\ & \left(\frac{\mathrm{d}^2}{\mathrm{d}s^2} + \frac{1}{s}\frac{\mathrm{d}}{\mathrm{d}s} - \frac{n^2}{s^2}\right)F(s) = F(s). \end{aligned} \tag{39}$$

The solutions are $I_{\pm n}(s)$ (regular as $s \to 0$) and $K_n(s)$ (regular as $s \to \infty$). If n is an integer, then I_n and I_{-n} are not linearly independent.

Recurrence relations if $F_n(s)=I_n(s)$ or $\exp(in\pi)K_n(s)$ ($=(-1)^n K_n(s)$ for n integral):

$$\begin{array}{ll} F_{n-1}(s) - F_{n+1}(s) = \dfrac{2n}{s}F_n(s) & F_{n-1}(s) - \dfrac{n}{s}F_n(s) = \dfrac{\mathrm{d}F_n}{\mathrm{d}s} \\ F_{n-1}(s) + F_{n+1}(s) = 2\dfrac{\mathrm{d}F_n}{\mathrm{d}s} & F_{n+1}(s) + \dfrac{n}{s}F_n(s) = \dfrac{\mathrm{d}F_n}{\mathrm{d}s} \end{array}. \tag{40}$$

2.2 Series solutions for small arguments:

$$\begin{aligned} I_n(s) &= \left(\frac{s}{2}\right)^n \sum_{k=0}^{\infty}\left(\frac{s^2}{4}\right)^k \frac{1}{k!\,\Gamma(n+k+1)}: \quad \text{for integral } n,\ \Gamma(n+1) = n! \\ K_n(s) &= \frac{1}{2}\left(\frac{s}{2}\right)^{-n} \sum_{k=0}^{n-1}\left(\frac{-s^2}{4}\right)^k \frac{(n-k-1)!}{k!} + (-1)^{n+1}\ln\left(\frac{s}{2}\right)I_n(s) \ + \cdots \\ &\quad + (-1)^n \frac{1}{2}\left(\frac{s}{2}\right)^n \sum_{k=0}^{\infty}\left(\frac{s^2}{4}\right)^k \frac{\Psi(n+k+1)+\Psi(k+1)}{k!(n+k)!} \\ \Psi(n) &= -\gamma + \sum_{k=1}^{n-1}\left(\frac{1}{k}\right), \quad \text{with } \Psi(1) = -\gamma = \lim_{m\to\infty}\left(1+\frac{1}{2}+\ldots+\frac{1}{m}-\ln(m)\right) = -0.57721\ 56649 \end{aligned} \tag{41}$$

Particular series needed here are:

$$
\begin{aligned}
I_0(s) &= 1+\left(\frac{s^2}{4}\right)\frac{1}{(1!)^2}+\left(\frac{s^2}{4}\right)^2\frac{1}{(2!)^2}+\left(\frac{s^2}{4}\right)^3\frac{1}{(3!)^2}+\ldots \\
I_1(s) &= \left(\frac{s}{2}\right)\left[1+\left(\frac{s^2}{4}\right)\frac{1}{2}+\left(\frac{s^2}{4}\right)^2\frac{1}{2!3!}+\left(\frac{s^2}{4}\right)^3\frac{1}{3!4!}+\ldots\right] \\
K_0(s) &= -\left[\gamma+\ln\left(\frac{s}{2}\right)\right]I_0(s)+\left(\frac{s^2}{4}\right)\frac{1}{(1!)^2}+\left(\frac{s^2}{4}\right)^2\frac{(1+1/2)}{(2!)^2}+\left(\frac{s^2}{4}\right)^3\frac{(1+1/2+1/3)}{(3!)^2}+\ldots \\
K_1(s) &= \frac{1}{s}+\left[\gamma+\ln\left(\frac{s}{2}\right)\right]I_1(s)-\left(\frac{s}{4}\right)\left[1+\left(\frac{s^2}{4}\right)\frac{5/2}{2}+\left(\frac{s^2}{4}\right)^2\frac{10/3}{2!3!}+\left(\frac{s^2}{4}\right)^3\frac{47/12}{3!4!}+\ldots\right].
\end{aligned}
\tag{42}
$$

2.3 Series expansions for large arguments:

$$
\begin{aligned}
I_n(s) &= \frac{\exp(s)}{\sqrt{2\pi s}}\left[1-\frac{\mu-1}{8s}+\frac{(\mu-1)(\mu-9)}{2!(8s)^2}-\frac{(\mu-1)(\mu-9)(\mu-25)}{3!(8s)^3}+\ldots\right] \\
K_n(s) &= \sqrt{\frac{\pi}{2s}}\exp(-s)\left[1+\frac{\mu-1}{8s}+\frac{(\mu-1)(\mu-9)}{2!(8s)^2}+\frac{(\mu-1)(\mu-9)(\mu-25)}{3!(8s)^3}+\ldots\right]
\end{aligned}
\tag{43}
$$

$\mu = 4n^2$

The particular series needed in this work are:

$$
\begin{aligned}
I_0(s) &= \frac{\exp(s)}{\sqrt{2\pi s}}\left[1+\frac{1}{8s}+\frac{9}{2(8s)^2}+\frac{75}{2(8s)^3}+\frac{75\times 49}{8(8s)^4}+\ldots\right] \\
I_1(s) &= \frac{\exp(s)}{\sqrt{2\pi s}}\left[1-\frac{3}{8s}-\frac{15}{2(8s)^2}-\frac{105}{2(8s)^3}-\frac{105\times 45}{8(8s)^4}+\ldots\right] \\
K_0(s) &= \sqrt{\frac{\pi}{2s}}\exp(-s)\left[1-\frac{1}{8s}+\frac{9}{2(8s)^2}-\frac{75}{2(8s)^3}+\frac{75\times 49}{8(8s)^4}+\ldots\right] \\
K_1(s) &= \sqrt{\frac{\pi}{2s}}\exp(-s)\left[1+\frac{3}{8s}-\frac{15}{2(8s)^2}+\frac{105}{2(8s)^3}-\frac{105\times 45}{8(8s)^4}+\ldots\right].
\end{aligned}
\tag{44}
$$

2.4 Function plots

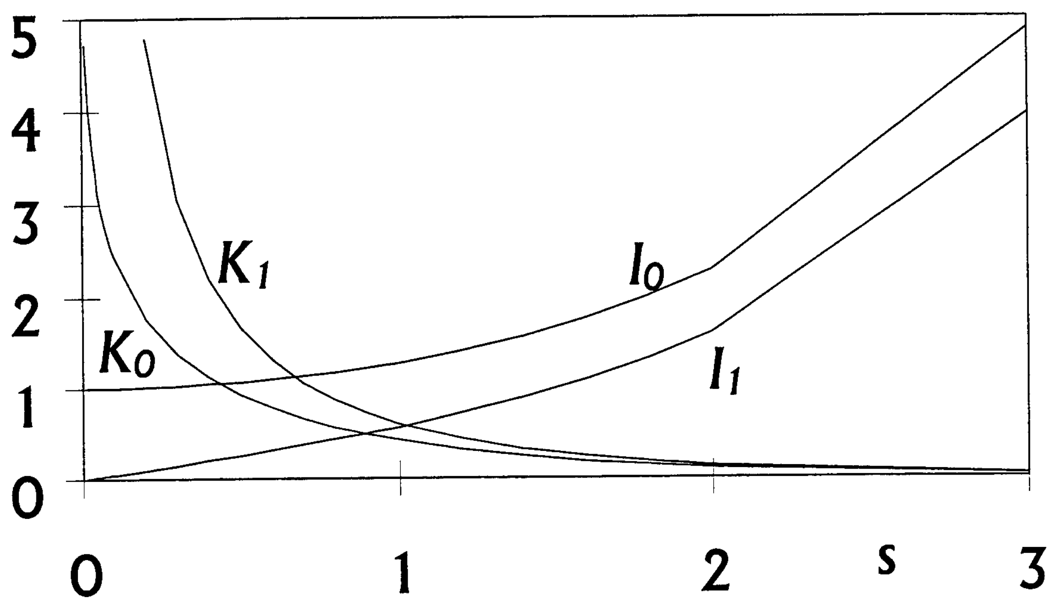

Figure 10 Plot of the low order modified Bessel functions. Note that I_0 and I_1 are finite for $s \to 0$ while K_0 and K_1 $\to 0$ as $s \to \infty$.

2.5 Polynomial representations

There are polynomial representations for these functions, together with their accuracy. These expressions were used in calculation when the argument precluded use of the above large or small argument approximations. In all of the following series, the expansion of the indicated function is $C_0 + C_1 t + C_2 t^2 + C_3 t^3 + \ldots$

Table 2 Coefficients in polynomial approximations to the modified Bessel functions I_0 and I_1.

Function	$I_0(s)$	$\sqrt{s}\exp(-s)I_0(s)$	$s^{-1}I_1(s)$	$\sqrt{s}\exp(-s)I_1(s)$
Applicable domain	$s<3.75$	$s\geq3.75$	$s<3.75$	$s\geq3.75$
Expansion variable t	$t=(s/3.75)^2$	$t=3.75/s$	$t=(s/3.75)^2$	$t=3.75/s$
C_0	1.0000000	0.39894228	0.50000000	0.39894228
C_1	3.5156229	0.01328592	0.87890594	-0.03988024
C_2	3.0899424	0.00225319	0.51498869	-0.00362018
C_3	1.2067492	-0.00157565	0.15084934	0.00163801
C_4	0.2659732	0.00916281	0.02658733	-0.01031555
C_5	0.0360768	-0.02057706	0.00301532	0.02282967
C_6	0.0045813	0.02635537	0.00032411	-0.02895312
C_7		-0.01647633		0.01787654
C_8		0.00392377		-0.00420059
maximum |error|	1.6×10^{-7}	1.9×10^{-7}	8×10^{-9}	2.2×10^{-7}

Table 3 Coefficients in polynomial approximations to the modified Bessel functions K_0 and K_1.

Function	$K_0(s)$	$\sqrt{s}\exp(s)K_0(s)$	$sK_1(s)$	$\sqrt{s}\exp(s)K_1(s)$
Applicable domain	$s<2$	$s\geq 2$	$s<2$	$s\geq 2$
Expansion variable t	$t=(s/2)^2$	$t=2/s$	$t=(s/2)^2$	$t=2/s$
Added function	$-\ln(s/2)\,I_0(s)$		$s\ln(s/2)\,I_1(s)$	
C_0	-0.57721566	1.25331414	1.00000000	1.25331414
C_1	0.42278420	-0.07832358	0.15443144	0.23498619
C_2	0.23069756	0.02189568	-0.67278579	-0.03655620
C_3	0.03488590	-0.01062446	-0.18156897	0.01504268
C_4	0.00262698	0.00587872	-0.01919402	-0.00780353
C_5	0.00010750	-0.00251540	-0.00110404	0.00325614
C_6	0.00000740	0.00053208	-0.00004686	-0.00068245
maximum |error|	1×10^{-8}	1.9×10^{-7}	8×10^{-9}	2.2×10^{-7}

3. Appendix 3: Parameters for a typical bonded composite reinforcement of an aluminium panel

3.1 Input geometrical parameters

Table 4 Geometric parameters for a typical bonded reinforcement repair.

Parameter	Symbol (Unit)	Plate (P) (Aluminium)	Adhesive (A) (FM 73)	Reinforcement (R) (10 ply boron)
Young's modulus	E (GPa)	72.4	1.89	207
Shear modulus	μ (GPa)	27.22	0.70	79.62
Poisson's ratio	ν	0.33	0.35	0.30
Thickness	t (mm)	3.10	0.10	1.27

3.2 Calculated and other input parameters

Table 5 Other parameters and those derived from the above.

Parameter	Unit	Formula	Values
$\sigma_{rr}^{P,\infty}$	MPa	Remote plate stress	100
$\sigma_{rr}^{R\infty}$	MPa	$\left(\frac{1-\nu_P}{1-\nu_R}\right)\left(\frac{1+\nu_R}{1+\nu_P}\right)\frac{\mu_R}{\mu_P}\sigma_{rr}^{P,\infty}$	273.7
γ		$-\lim_{m\to\infty}\left(1+\frac{1}{2}+\ldots+\frac{1}{m}-\ln(m)\right)$	0.577216
g_R	1/(mmMPa)	$(1-\nu_R)/(t_R\mu_R)=2(1-\nu_R^2)/(t_RE_R)$	0.006923
g_P	1/(mmMPa)	$(1-\nu_P)/(t_P\mu_P)=2(1-\nu_P^2)/(t_PE_P)$	0.007941
γ_R		$g_R/(g_R+g_P)$	0.4658
γ_P		$g_P/(g_R+g_P)$	0.5342

β_r^2	1/(mm)^2	$(\mu_A/t_A)\times(g_R+g_P)$	0.05202
β_θ^2	1/(mm)^2	$2(\mu_A/t_A)\times(1/t_R\mu_R+1/t_P\mu_P)$	0.15219
β_r	1/(mm)	$\sqrt{\beta_r^2}$	0.2281
β_θ	1/(mm)	$\sqrt{\beta_\theta^2}$	0.3901
β_r^{-1}	mm	$1/\beta_r$	4.3843
h		$\frac{2-(1+\nu_P)\gamma_R}{2(1-\nu_P)}$	1.0302

3.3 Calculations of SCF at two hole radii

Table 6 Parameters in the calculation of the stress concentration factor for the typical bonded repair and hole radii of 1mm and 10mm.

Parameter	Formula	R=1mm	R=10mm
s_R	$\beta_r R$	0.2281	2.2809
$K_0(s_R)$	Bessel function	1.6278	0.08098
$K_1(s_R)$	Bessel function	4.1434	0.09732
$F_K(s_R)$	$s_R K_0(s_R)/K_1(s_R)$	0.08961	1.8979
$SCF(s_R)$	$\frac{2+F_K(s_R)}{1+hF_K(s_R)}$	1.9130	1.3189

3.4 Standard and normalised constants for the displacement formulae

Equations 13 and 14:

$$u_r^R(s>s_R)=C_1^R s+C_{-1}^R/s+\gamma_R BK_1(s)$$
$$u_r^P(s>s_R)=C_1^R s+C_{-1}^R/s-\gamma_P BK_1(s).$$
$$u_r^{R,-}(s<s_R)=D_1^R s$$

Table 7 Parameters calculated for the displacement functions reproduced above.

Constant		R=1mm		R=10mm	
Standard	Normalised	Standard	Normalised	Standard	Normalised
C_1^R	$\beta_r C_1^R$	4.0573	0.9254	4.0573	0.9254
C_{-1}^R	C_{-1}^R/β_r	0.1867	0.8184	12.87	56.426
D_1^R	$\beta_r D_1^R$	4.2112	0.9605	5.2619	1.2002
B	B/β_r	-0.4059	-1.7795	-63.872	-280.03

DISTRIBUTION LIST

Stress Concentration Around a Patched Hole in an Axi-Symmetrically Loaded Plate

C. Pickthall, and L. R. F. Rose

AUSTRALIA

TASK SPONSOR: AIR OIC ASI-LSA

DEFENCE ORGANISATION

Defence Science and Technology Organisation

Chief Defence Scientist
FAS Science Policy
AS Science Corporate Management
} shared copy
Counsellor Defence Science, London (Doc Data Sheet only)
Counsellor Defence Science, Washington (Doc Data Sheet only)
Scientific Adviser to the MDRC (Doc Data Sheet only)
Director General Science Policy Development
Senior Defence Scientific Adviser/ Scientific Adviser Policy and Command (shared copy)
Navy Scientific Adviser (Doc Data Sheet and distribution list)
Scientific Adviser - Army (Doc Data Sheet and distribution list)
Air Force Scientific Adviser
Director Trials

Aeronautical and Maritime Research Laboratory

Director
Chief of Division (AED)
Research Leader Fracture Mechanics
Task Manager (Chun Wang)
Author(s):
C.R. Pickthall (5 copies)
L.R.F. Rose
R. Bartholomeusz

DSTO Library

Library Fishermens Bend
Library Maribyrnong
Main Library DSTOS (2 copies)
Library, MOD, Pyrmont (Doc Data sheet)
Australian Archives

Corporate Support Program

OIC TRS, Defence Regional Library, Canberra
Officer in Charge, Document Exchange Centre (DEC), (Doc Data sheet)
DEC requires the following copies of public release reports to meet exchange agreements under their management:
* US Defence Technical Information Centre, 2 copies
* UK Defence Research Information Centre, 2 copies
* Canada Defence Scientific Information Service, 1 copy
* NZ Defence Information Centre, 1 copy

National Library of Australia, 1 copy

Intelligence Program
DGSTA, Defence Intelligence Organisation

Capability Development Division
Director General Maritime Development (Doc Data sheet)
Director General C3I Development (Doc Data sheet)
Director General Land Development (Doc Data sheet)

Army

ABCA Office, G-1-34, Russell Offices, Canberra (4 copies)

UNIVERSITIES AND COLLEGES

Australian Defence Force Academy
Library
Head of Aerospace and Mechanical Engineering
Deakin University, Serials Section (M list)), Deakin University Library
Senior Librarian, Hargrave Library, Monash University

OTHER ORGANISATIONS

NASA (Canberra)
AGPS

ABSTRACTING AND INFORMATION ORGANISATIONS
INSPEC: Acquisitions Section Institution of Electrical Engineers
Library, Chemical Abstracts Reference Service
Engineering Societies Library, US
American Society for Metals
Documents Librarian, The Center for Research Libraries, US

INFORMATION EXCHANGE AGREEMENT PARTNERS
Acquisitions Unit, Science Reference and Information Service, UK
Library - Exchange Desk, National Institute of Standards and Technology, US
National Aerospace Laboratory, Japan
National Aerospace Laboratory, Netherlands

SPARES (5 copies)

Total Number of Copies: 55

Page classification: UNCLASSIFIED

DEFENCE SCIENCE AND TECHNOLOGY ORGANISATION DOCUMENT CONTROL DATA	1. PRIVACY MARKING/CAVEAT (OF DOCUMENT)

2. TITLE Stress Concentration Around a Patched Hole in an Axi-Symmetrically Loaded Plate	3. SECURITY CLASSIFICATION (FOR UNCLASSIFIED REPORTS THAT ARE LIMITED RELEASE USE (L) NEXT TO DOCUMENT CLASSIFICATION) Document (U) Title (U) Abstract (U)
4. AUTHOR(S) C. Pickthall, and L. R. F. Rose	5. CORPORATE AUTHOR Aeronautical and Maritime Research Laboratory PO Box 4331 Melbourne Vic 3001

6a. DSTO NUMBER DSTO-RR-0132	6b. AR NUMBER AR-010-543	6c. TYPE OF REPORT Research Report	7. DOCUMENT DATE June, 1998

8. FILE NUMBER M1/9/269	9. TASK NUMBER 95/228	10. TASK SPONSOR AIR OIC ASI-LSA	11. NO. OF PAGES 23	12. NO. OF REFERENCES 4

13. DOWNGRADING/DELIMITING INSTRUCTIONS To be reviewed three years after date of publication	14. RELEASE AUTHORITY Chief, Airframes and Engines Division

15. SECONDARY RELEASE STATEMENT OF THIS DOCUMENT
16.

Approved for public release

OVERSEAS ENQUIRIES OUTSIDE STATED LIMITATIONS SHOULD BE REFERRED THROUGH DOCUMENT EXCHANGE CENTRE, DIS NETWORK OFFICE, DEPT OF DEFENCE, CAMPBELL PARK OFFICES, CANBERRA ACT 2600

16. DELIBERATE ANNOUNCEMENT

No limitations

17. CASUAL ANNOUNCEMENT Yes

18. DEFTEST DESCRIPTORS

adhesive bonding, repair, stress analysis, fatigue tests, stress concentration

19. ABSTRACT

This paper examines the efficiency of an adhesively bonded reinforcement patch in reducing the stress concentration around a hole in a plate, as a function of hole size. Differential equations are derived for the radial and tangential displacements in the plate and reinforcement assuming only in-plane stresses without out-of-plane bending. Imposition of angular independence leads to distinct load transfer lengths for radial and tangential adhesive shear (β_r^{-1} and β_θ^{-1} respectively), and zero tangential displacement reduces the problem to a patched circular hole with axi-symmetric loading. Four boundary conditions permitted analytic solutions in terms of modified Bessel functions. A stress concentration factor (*SCF*) is defined as the tangential stress in the plate at the hole boundary, compared to that far away in the plate but still under the reinforcement. Plotting *SCF* against hole radius normalised by β_r^{-1}, leads to an analytic function with a single (non-dimensional) parameter h, depending on the thicknesses and moduli of the components. *SCF* approaches two in the limit of small holes indicating that the reinforcement is ineffective in that limit. *SCF* approaches $1/h$ in the large-hole limit. For the typical repair geometry where $h \approx 1$, *SCF* falls to 1.6 when the hole radius reaches β_r^{-1}, and 1.3 by $3\beta_r^{-1}$. The related problem of a circular reinforcement bonded on a large (unholed) plate is briefly examined. This indicates how the normalisation stress for *SCF* relates to that applied beyond the patch.

Page classification: UNCLASSIFIED